

A Finite Element Formulation of Baraff-Witkin Cloth

Theodore Kim
Yale University

Abstract

The Baraff-Witkin [BW98] model has been a popular formulation for cloth for 20 years. However, its relationship to the finite element method (FEM) has always been unclear, because the model resists being written as an isotropic, hyperelastic strain energy. In this paper, we show that this is because the Baraff-Witkin model is actually a coupled anisotropic strain energy. We show that its stretching term approximates the isotropic As-Rigid-As-Possible (ARAP) energy, and its shearing term is a cross-fiber coupling energy common in biomechanics. While it has been known empirically for some time that the model can produce indefinite force Jacobians, the conditions under which they occur has never been clear. Our formulation enables a complete eigenanalysis that precisely characterizes exactly when indefiniteness occurs, and leads to fast, analytic, semi-positive-definite projection methods. Finally, our analysis suggests a generalized Baraff-Witkin energy with non-orthogonal warp and weft directions.

1. Introduction

The Baraff-Witkin model for cloth [BW98] has been widely used in film for almost 20 years. First appearing on-screen in *Monsters, Inc.* in 2001, it has been the workhorse cloth model for every subsequent Pixar film [Ebe18], and is widely used at Walt Disney Animation Studios (see e.g. [TJM15]).

Despite the popularity and ubiquity of this model, ambiguity persists around some of its main features. Most contemporary solid mechanics simulations in computer graphics rely on the finite element method (FEM) [SGK18], position based dynamics [MHHR07], or a spring-mass formulation [CK02]. However, the Baraff-Witkin model inhabits a liminal space in between. Much like position based dynamics (which it arguably inspired), the model is written in terms of constraint functions. At the same time, the constraint functions appear very spring-mass-like, even though the formulation is face-based, not edge-based. Finally, the model forms an FEM-like globally implicit system, even though finite element shape functions and their derivatives are never explicitly invoked.

In this paper, we show that the Baraff-Witkin model can be understood entirely in terms of FEM. The first step in such an analysis is usually to write the model as an isotropic, hyperelastic strain energy [BW08]. However, it has never been clear how to do this for the Baraff-Witkin model. We show that an isotropic formulation is impossible, but that a *coupled anisotropic* strain energy can be both formulated and analyzed using a recent approach [KDG119].

Using this energy, we are able to establish that the Baraff-Witkin stretching term is an anisotropic approximation of the isotropic As-Rigid-As-Possible (ARAP) energy from geometry processing [SA07], which is itself a spring-mass-like energy. Subsequently, we show that the Baraff-Witkin shearing term corresponds directly



Figure 1: **Left:** Results using our finite element formulation of Baraff-Witkin cloth. **Right:** Same scene, but with ARAP stretching. The ARAP results appear more rubber-like, as higher frequency wrinkling is slightly suppressed, and a characteristic low frequency wrinkle appears down the middle. In both, $k = 250$ and $k_{\theta} = 1e^{-8}$.

to the cross-fiber shearing term that commonly appears in muscles in biomechanics [CDH01, BPD05].

Finally, we use this energy formulation to characterize the exact conditions under which the Baraff-Witkin model produces indefinite systems. This indefiniteness is not mentioned in the original paper [BW98], but has been known empirically for some time (see e.g. §3.1 in [CK02] or [MFG09]). We perform a novel eigenanalysis that quantitatively establishes the exact conditions under which indefiniteness occurs using the Bunch-Nielsen-Sorensen formula [BNS78]. We obtain closed-form, analytic expressions for the eigenvalues and eigenvectors of each triangle, which allow us to construct a fast, simple, and analytic methods for projecting the systems back to semi-positive-definiteness. We demonstrate the efficacy of our formulation in a variety of scenarios (Figs. 1,2,4).

In summary, our contributions are:

- An anisotropic FEM energy for the Baraff-Witkin cloth model
- A complete eigenanalysis of the energy, including a novel approach using the Bunch-Nielsen-Sorensen formula
- An analysis showing that the energy is an anisotropic approximation of the isotropic ARAP energy
- A fast, analytic semi-positive-definiteness projection method.
- A generalized Baraff-Witkin energy with non-orthogonal warp and weft directions.

2. Related Works

The original Baraff and Witkin [BW98] paper is cited for many reasons, including its constraint-based energies, its popularization of preconditioned conjugate gradients (PCG), and its use of backward Euler. In this work, we will focus on the constitutive model it uses for in-plane stretching and shearing.

Many such models have been used in the past, such as mass-spring [Pro95, VT00, CK02, BFA02], St. Venant Kirchhoff (StVK) [MMO16], Kirchhoff-Love [CTT17, CSvRV18], corotational [EKS03], piecewise linear [WOR11] and linear orthotropic models [VMTF09, LB15]. Additional non-linear constraints can be incorporated using strain limiting [TPS09], where the authors also closely examine the role of shearing. An in-depth comparison, in the context of data-driven simulation, between spring-mass, Baraff-Witkin, and FEM-based StVK models is also available [MBT*12]. Of all these works, the orthotropic model is the closest to the results we present here, though our invariant-based analysis also applies to more general anisotropic (Appendix B) and non-linear models.

The Baraff-Witkin model was not originally presented as an FEM model, resulting in many works over the last two decades[†] mistakenly classifying it as a mass-spring model. Its constraint-based formulation also served as inspiration for position-based [MHHR07, BMO*14] and projective dynamics [BML*14, NOB16], which has further muddied attempts at classification. As part of this work, we hope to certify Baraff-Witkin as an FEM model and dispel any lingering ambiguity.

The effectiveness of PCG in the original paper [BW98] is contingent on the underlying energies producing semi-positive-definite systems, but in the years since, they have been observed to produce indefinite systems [CK02, MFG09]. The issue can be broadly addressed by applying the Gauss-Newton approximation, which drops the second-order derivative from the force gradient [CK02], or more finely by filtering the eigenvalues at each quadrature point [TSIF05]. However, prior filtering methods only apply to isotropic Cauchy-Green [TSIF05] or transversely isotropic [KDG19] energies. Neither approach is sufficient for the Baraff-Witkin model, so we present a novel cross-fiber analysis (§4.3) that allows filtering to be applied analytically.

[†] Our original draft cited four such erroneous works, but we removed them upon revision. Instead, let us all focus on correctly classifying the model in the future.

3. The Baraff-Witkin Energies

3.1. The Original Formulation

We will begin with a brief overview of the original Baraff-Witkin formulation, following the notation of the original [BW98] as closely as possible. Once the preliminaries are established, we will show how to cast these into a finite element formulation.

The Baraff-Witkin approach uses a function $\mathbf{w}(u, v) \in \mathbb{R}^3$ to map from 2D material-space to 3D world-space. Deformation is then measured using the gradient of $\mathbf{w}(u, v)$, denoted

$$\mathbf{w}_u = \frac{\partial \mathbf{w}(u, v)}{\partial u} \in \mathbb{R}^3 \quad \mathbf{w}_v = \frac{\partial \mathbf{w}(u, v)}{\partial v} \in \mathbb{R}^3. \quad (1)$$

The in-plane (u, v) coordinates and the current world-space triangle vertices $\mathbf{x}_{i,j,k}$ are combined to obtain \mathbf{w}_u and \mathbf{w}_v thusly:

$$\begin{aligned} \begin{bmatrix} \mathbf{w}_u & \mathbf{w}_v \end{bmatrix} &= \begin{bmatrix} \mathbf{x}_j - \mathbf{x}_i & \mathbf{x}_k - \mathbf{x}_i \end{bmatrix} \begin{bmatrix} u_j - u_i & u_k - u_i \\ v_j - v_i & v_k - v_i \end{bmatrix}^{-1} \\ &= \begin{bmatrix} \Delta \mathbf{x}_1 & \Delta \mathbf{x}_2 \end{bmatrix} \begin{bmatrix} \Delta u_1 & \Delta u_2 \\ \Delta v_1 & \Delta v_2 \end{bmatrix}^{-1} \in \mathbb{R}^{3 \times 2}. \end{aligned} \quad (2)$$

Baraff and Witkin use this gradient to define stretching and shearing energies that model in-plane forces. These are respectively:

$$E_{\text{stretch}} = a \left[(\|\mathbf{w}_u\| - b_u)^2 + (\|\mathbf{w}_v\| - b_v)^2 \right] \quad (4)$$

$$E_{\text{shear}} = a \left(\mathbf{w}_u^\top \mathbf{w}_v \right)^2. \quad (5)$$

Above, $\|\cdot\|$ denotes the 2-norm, a is the triangle area, and b_u and b_v are shrink/stretch parameters that are usually set to one.

3.2. No Isotropic FEM Formulation Exists

FEM practitioners will immediately see that $[\mathbf{w}_u \ \mathbf{w}_v]$ corresponds to the deformation gradient $\mathbf{F} \in \mathbb{R}^{3 \times 2}$, but that shape function derivatives, which usually appear in a change-of-variables tensor $\frac{\partial \mathbf{F}}{\partial \mathbf{x}}$, are absent. Instead, forces are computed using positional derivatives, $\mathbf{f} = -k \frac{\partial E_{\text{stretch}}}{\partial \mathbf{x}}$, where k is a stiffness constant.

The usual FEM process is to formulate Ψ , a strain energy density akin to E_* , and compute forces using $\mathbf{f} = -ka \frac{\partial \Psi}{\partial \mathbf{x}}$. (Again, k is a stiffness and a is area.) However, Ψ is usually written in terms of \mathbf{F} instead of \mathbf{x} , so we initially compute the first Piola-Kirchhoff tensor (PK1) $\frac{\partial \Psi}{\partial \mathbf{F}}$, and then convert it to $\frac{\partial \Psi}{\partial \mathbf{x}}$ using a change of variables,

$$\mathbf{f} = -ka \frac{\partial \Psi}{\partial \mathbf{x}} = -ka \frac{\partial \mathbf{F}}{\partial \mathbf{x}} : \frac{\partial \Psi}{\partial \mathbf{F}}, \quad (6)$$

where $:$ is a double-contraction because $\frac{\partial \mathbf{F}}{\partial \mathbf{x}} \in \mathbb{R}^{3 \times 2 \times 9}$ is a 3rd-order tensor. In this way, the $\frac{\partial \mathbf{F}}{\partial \mathbf{x}}$ shape function derivatives are introduced into the computation.

However, it is not obvious how to formulate a Ψ for E_{stretch} and E_{shear} , because they are written with respect to \mathbf{w}_u and \mathbf{w}_v , which are the *columns* of \mathbf{F} . It is well-known [BW08] that all isotropic FEM energies can be written using the Cauchy-Green invariants,

$$I_C = \text{tr}(\mathbf{F}^\top \mathbf{F}) \quad II_C = \text{tr}(\mathbf{F}\mathbf{F}^\top \mathbf{F}^\top \mathbf{F}) \quad III_C = \det(\mathbf{F}^\top \mathbf{F}) \quad (7)$$

or a recent set of more general invariants [SGK19]:

$$I_1 = \text{tr}(\mathbf{S}) \quad I_2 = \text{tr}(\mathbf{S}^T \mathbf{S}) \quad I_3 = \det(\mathbf{S}), \quad (8)$$

where \mathbf{S} denotes the stretch matrix from the polar decomposition $\mathbf{F} = \mathbf{R}\mathbf{S}$. However, the Baraff-Witkin energies *cannot be written using these*, because all of these invariants entangle the columns of \mathbf{F} . The column-wise separation required by E_{stretch} and E_{shear} is not supported. These invariants encompass all possible isotropic FEM energies, so we must conclude that it is *impossible* to write the Baraff-Witkin model as an isotropic FEM energy.

3.3. An Anisotropic FEM Formulation Exists

Instead, we show that it is possible to write E_{stretch} and E_{shear} as *anisotropic* FEM energies. Such materials are common in biomechanics for modeling muscle fibers [CRF15], but here they will be used to express woven fiber directions.

In addition to the isotropic invariants in Eqn. 8, there are also anisotropic invariants [KDG19]

$$I_4(\mathbf{a}) = \mathbf{a}^T \mathbf{S} \mathbf{a} \quad I_5(\mathbf{a}) = \mathbf{a}^T \mathbf{F}^T \mathbf{F} \mathbf{a}, \quad (9)$$

where $\mathbf{a} \in \mathfrak{R}^2$ is an anisotropy direction in 2D material-space.

Crucially, if we use the standard basis directions, $\mathbf{a}_u = [1 \ 0]^T$ and $\mathbf{a}_v = [0 \ 1]^T$ in the I_5 invariant, we obtain the *exact column-wise separation* that was missing from the isotropic invariants. To illustrate this, we label the columns of \mathbf{F} as

$$\mathbf{F} = \begin{bmatrix} \mathbf{f}_0 & \mathbf{f}_1 \end{bmatrix}. \quad (10)$$

Then, $\mathbf{F}\mathbf{a}_u = \mathbf{f}_0$ and $I_5(\mathbf{a}_u) = (\mathbf{F}\mathbf{a}_u)^T \mathbf{F}\mathbf{a}_u = \|\mathbf{f}_0\|^2$, which corresponds to $\|\mathbf{w}_u\|^2$. The $\|\mathbf{w}_u\|$ term from Eqn. 4 can now be written in invariant form as $\sqrt{I_5(\mathbf{a}_u)}$. The full anisotropic FEM stretching energy becomes:

$$\Psi_{\text{stretch}} = \left[\left(\sqrt{I_5(\mathbf{a}_u)} - b_u \right)^2 + \left(\sqrt{I_5(\mathbf{a}_v)} - b_v \right)^2 \right]. \quad (11)$$

We have dropped a because Ψ denotes an energy density, so the area gets re-introduced by Eqn. 6.

To express E_{shear} , an additional *cross-fiber* invariant is needed:

$$I_6(\mathbf{a}, \mathbf{b}) = \mathbf{a}^T \mathbf{F}^T \mathbf{F} \mathbf{b}, \quad (12)$$

where $\mathbf{a} \neq \mathbf{b}$ in general. This invariant is important in biomechanics [BPD05], but was discounted in recent graphics work [KDG19] because its visual relevance was unclear. While the relevance in 3D solids may be subtle, we will see in §5 that it plays a critical role in the qualitative behavior of cloth. Using this invariant, the shearing energy can be written

$$\Psi_{\text{shear}} = I_6(\mathbf{a}_u, \mathbf{a}_v)^2. \quad (13)$$

We now have two expressions for Baraff-Witkin cloth, Eqns. 11 and 13, that are expressed entirely as invariant-based FEM energies. Using these, we can now establish connections to other FEM energies (§3.4), and perform an eigenanalysis (§4) to better understand their quantitative behavior.

3.4. Baraff-Witkin Stretching Approximates ARAP

We can show that Ψ_{stretch} is an anisotropic approximation of the element-wise formulation of the As-Rigid-As-Possible (ARAP) energy [LZX*08, CPSS10]:

$$\Psi_{\text{ARAP}} = \|\mathbf{F} - \mathbf{R}\|_F^2. \quad (14)$$

Expanding the Frobenius norm yields,

$$\Psi_{\text{ARAP}} = I_2 - 2I_1 + 2, \quad (15)$$

where I_2 and I_1 are the invariants from Eqn. 8.

Performing a similar expansion of Ψ_{stretch} yields

$$\begin{aligned} \Psi_{\text{stretch}} &= I_5(\mathbf{u})^2 + I_5(\mathbf{v})^2 - 2 \left(\sqrt{I_5(\mathbf{u})} + \sqrt{I_5(\mathbf{v})} \right) + 2 \quad (16) \\ &= I_2 - 2 \left(\sqrt{I_5(\mathbf{u})} + \sqrt{I_5(\mathbf{v})} \right) + 2. \quad (17) \end{aligned}$$

The second line uses the identity $I_5(\mathbf{u})^2 + I_5(\mathbf{v})^2 = \|\mathbf{F}\|_F^2 = I_2$, and we have set $b_u = b_v = 1$ for this comparison.

Comparing Eqns. 15 and 17, the core approximation is clearly

$$I_1 \approx \sqrt{I_5(\mathbf{a}_u)} + \sqrt{I_5(\mathbf{a}_v)}. \quad (18)$$

When $\mathbf{U} = \mathbf{V} = \mathbf{I}$ in the SVD $\mathbf{F} = \mathbf{U}\mathbf{\Sigma}\mathbf{V}^T$, this matches up to sign change. The approximation $I_1 \approx \sqrt{I_5(\mathbf{a}_u)} + \sqrt{I_5(\mathbf{a}_v)}$ becomes

$$\sigma_0 + \sigma_1 \approx |\sigma_0| + |\sigma_1|, \quad (19)$$

where σ_0 and σ_1 are the singular values of \mathbf{F} . For shells, a negative singular value corresponds to out-of-plane π -rotation, so the match in this case is exact for all practical purposes.

Therefore, the Baraff-Witkin stretching energy is an ARAP-like energy that principally resists stretching in the \mathbf{a}_u and \mathbf{a}_v directions instead of the time-varying principal directions that arise from the SVD of \mathbf{F} . This model is consistent with cloth, which is persistently stiffer along the threads in the orthogonal warp and weft directions. In §5, we will examine the visual differences between the ARAP and Baraff-Witkin energies, and obtain some novel qualitative behaviors by relaxing the orthogonality assumption.

4. An Eigenanalysis of Baraff-Witkin Cloth

4.1. Analysis Preliminaries

We will now show how to obtain closed-form, analytic expressions for the eigensystems of Ψ_{stretch} and Ψ_{shear} , which we can then use to determine when the energies become indefinite.

As shown in previous works [SGK19, KDG19], analyzing the energy Hessian $\partial^2\Psi/\partial\mathbf{F}^2$ in lieu of the force Jacobian can reveal simple expressions for the eigensystems of various energies. The Hessian can later be converted back to the force Jacobians using

$$\frac{\partial \mathbf{f}}{\partial \mathbf{x}} = \mathbf{a} \cdot \text{vec} \left(\frac{\partial \mathbf{F}}{\partial \mathbf{x}} \right)^T \text{vec} \left(\frac{\partial^2 \Psi}{\partial \mathbf{F}^2} \right) \text{vec} \left(\frac{\partial \mathbf{F}}{\partial \mathbf{x}} \right)^T, \quad (20)$$

where $\text{vec}(\cdot)$ is a vectorization operator [GVL13, KDG19] that flattens higher-order tensors into 2nd-order matrices.

In the following, we will be making use of *eigenmatrices*. When using the 4th-order tensor $\partial^2\Psi/\partial\mathbf{F}^2$, the usual eigenvalue problem $\mathbf{A}\mathbf{q} = \lambda\mathbf{q}$ becomes $\partial^2\Psi/\partial\mathbf{F}^2 : \mathbf{Q} = \lambda\mathbf{Q}$. Thus, in lieu of the usual

eigenvectors \mathbf{q} , we obtain eigenmatrices \mathbf{Q} . While the two formulations are equivalent, we can perform decompositions such as the SVD on \mathbf{Q} to reveal structures that would be obscured by the vector form \mathbf{q} . In the following sections, we will present analytic eigenpairs of the form $(\lambda_i, \mathbf{Q}_i)$, but the eigenmatrix can always be converted back to an eigenvector by reordering the entries according to $\mathbf{q} = \text{vec}(\mathbf{Q})$.

4.2. The Stretching Energy Can Definitely Go Indefinite

4.2.1. The Eigensystem of Baraff-Witkin Stretching

Since Ψ_{stretch} is the sum of I_5 -based energies, and \mathbf{a}_u and \mathbf{a}_v are orthogonal, the six eigenpairs of its eigensystem can be obtained by applying §4.2 from [KDG19],

$$\lambda_0 = 2 \quad \mathbf{Q}_0 = \frac{1}{\|\mathbf{f}_0\|} \left[\begin{array}{c|c} \mathbf{f}_0 & \mathbf{0}_3 \end{array} \right] \quad (21)$$

$$\lambda_{1,2} = 2 \left(1 - \frac{b_u}{\sqrt{I_5(\mathbf{a}_u)}} \right) \quad \mathbf{Q}_{1,2} = \left[\begin{array}{c|c} \text{vectors} & \\ \text{orthogonal} & \\ \text{to } \mathbf{f}_0 & \mathbf{0}_3 \end{array} \right] \quad (22)$$

$$\lambda_3 = 2 \quad \mathbf{Q}_3 = \frac{1}{\|\mathbf{f}_1\|} \left[\begin{array}{c|c} \mathbf{0}_3 & \mathbf{f}_1 \end{array} \right] \quad (23)$$

$$\lambda_{4,5} = 2 \left(1 - \frac{b_v}{\sqrt{I_5(\mathbf{a}_v)}} \right) \quad \mathbf{Q}_{4,5} = \left[\begin{array}{c|c} \mathbf{0}_3 & \text{vectors} \\ & \text{orthogonal} \\ & \text{to } \mathbf{f}_1 \end{array} \right], \quad (24)$$

where $\mathbf{0}_3 \in \mathbb{R}^3$ is a vector of zeros.

Four of the eigenpairs, $\mathbf{Q}_{1,2}$ and $\mathbf{Q}_{4,5}$, have repeated eigenvalues, and thus span two arbitrary, rank-2 subspaces. We have not provided specific expressions for these eigenmatrices because they will not be needed for semi-positive-definiteness projection.

Baraff-Witkin stretching becomes indefinite when either $\lambda_{1,2}$ or $\lambda_{4,5}$ are negative, which occurs under the following conditions:

$$\sqrt{I_5(\mathbf{a}_u)} \leq b_u \quad \text{or} \quad \sqrt{I_5(\mathbf{a}_v)} \leq b_v. \quad (25)$$

Qualitatively, the stretching term becomes indefinite whenever the \mathbf{a}_u or \mathbf{a}_v directions *undergo compression*. The cloth enters a buckling regime where multiple energetically equivalent solutions exist [CK02], so the loss of convexity at this configuration is physically consistent.

4.2.2. Semi-Positive-Definite Projection

We can define a fast semi-positive-definite projection by first writing the vectorized Hessian, $\text{vec}(\partial^2 \Psi_{\text{stretch}} / \partial \mathbf{F}^2) = \mathbf{H}_{\text{stretch}}$, as follows,

$$\mathbf{H}_{\text{stretch}} = 2 \left[\begin{array}{c} \left(1 - \frac{1}{\sqrt{I_5(\mathbf{a}_u)}} \right) \mathbf{H}_u + \frac{1}{I_5(\mathbf{a}_u)^{\frac{3}{2}}} \mathbf{f}_0 \mathbf{f}_0^\top \\ \left(1 - \frac{1}{\sqrt{I_5(\mathbf{a}_v)}} \right) \mathbf{H}_v + \frac{1}{I_5(\mathbf{a}_v)^{\frac{3}{2}}} \mathbf{f}_1 \mathbf{f}_1^\top \end{array} \right],$$

where

$$\mathbf{H}_u = \begin{bmatrix} 1 & 0 \\ 0 & 0 \end{bmatrix} \otimes \mathbf{I}_{3 \times 3} \quad \mathbf{H}_v = \begin{bmatrix} 0 & 0 \\ 0 & 1 \end{bmatrix} \otimes \mathbf{I}_{3 \times 3}, \quad (26)$$

and \otimes is a Kronecker product. In the following, we will focus on filtering out negative eigenvalues in the u direction from the first line of $\mathbf{H}_{\text{stretch}}$, but the same reasoning applies to the v direction.

The $2(1 - 1/\sqrt{I_5(\mathbf{a}_u)}) \mathbf{H}_u$ term from $\mathbf{H}_{\text{stretch}}$ constructs a rank-3 subspace with all three non-zero eigenvalues pinned to $\lambda_{0,1,2} = 2(1 - b_u/\sqrt{I_5(\mathbf{a}_u)})$. Two of these can become negative, but the $2/I_5(\mathbf{a}_u)^{\frac{3}{2}} \mathbf{f}_0 \mathbf{f}_0^\top$ rank-1 update bumps a single eigenvalue from this subspace up to $\lambda_0 = 2$. In the case where the u direction is under compression, it is sufficient to zero out the \mathbf{H}_u matrix, and compute a modified rank-1 term, $2\mathbf{f}_0 \mathbf{f}_0^\top$ that still captures the $\lambda_0 = 2$ term. This approach is compact enough that we provide a complete C++ implementation in Appendix A.

This filter is similar to the Gauss-Newton approach of dropping the \mathbf{H}_u term [CK02]. However, that approach effectively clamps the eigenvalue to $\lambda_0 = 1/I_5(\mathbf{a}_u)^{\frac{3}{2}}$, which is closer to zero. The overall system then becomes both more poorly conditioned, and further away from the true Hessian.

4.2.3. Relationship to the ARAP Eigensystem

Using a recent analysis [Pan20], we can construct the analytic eigensystem for ARAP on a membrane, which is strikingly similar to Baraff-Witkin stretching. The first two eigenvalues are

$$\lambda_0^{\text{ARAP}} = 2 \left(1 - \frac{1}{\sigma_0} \right) \quad \lambda_1^{\text{ARAP}} = 2 \left(1 - \frac{1}{\sigma_1} \right), \quad (27)$$

while the remaining four are

$$\lambda_2^{\text{ARAP}} = 2 \left(1 - \frac{2}{\sigma_0 + \sigma_1} \right) \quad \lambda_{3,4,5}^{\text{ARAP}} = 2. \quad (28)$$

By setting $b_u = b_v = 1$ in Baraff-Witkin, and inserting the $\sigma_0 \approx \sqrt{I_5(\mathbf{a}_u)}$ and $\sigma_1 \approx \sqrt{I_5(\mathbf{a}_v)}$ approximations, Eqns. 22 and 24 can be brought into exact correspondence with Eqn. 27.

These correspond to the eigenvalues that can take on negative values, and while they form a rank-4 subspace in the Baraff-Witkin model (i.e. $\lambda_{1,2,4,5}$ in Eqns. 22 and 24), they only form a rank-2 subspace in ARAP ($\lambda_{0,1}^{\text{ARAP}}$ in Eqn. 27). The eigenvalue λ_2^{ARAP} can also become negative, but under stricter conditions: $\sigma_0 + \sigma_1 < 1$. Thus, ARAP can have a most a rank-3 negative-definite subspace, and is slightly more convex than Baraff-Witkin.

Finally, the λ_2^{ARAP} eigenvalue has no equivalent in Baraff-Witkin stretching, since the appearance of both singular values in an eigenvalue would correspond to a mixing of $I_5(\mathbf{a}_u)$ and $I_5(\mathbf{a}_v)$. But, Ψ_{stretch} prohibits this by construction. The natural conclusion is that Ψ_{shear} approximates this eigenpair, but as we will see next, this is not the case.

4.3. The Shearing Energy Is Always Indefinite

4.3.1. The Eigensystem of $I_6(\mathbf{a}, \mathbf{b})$

Obtaining the eigensystem of Ψ_{stretch} was a straightforward application of an existing analysis [KDG19] of $I_5(\mathbf{a})$. Unfortunately, no equivalent analysis exists for $I_6(\mathbf{a}, \mathbf{b})$, so we must provide it here.

The PK1 and vectorized Hessian of $I_6(\mathbf{a}, \mathbf{b})$ are as follows:

$$\frac{\partial I_6}{\partial \mathbf{F}} = \mathbf{F} (\mathbf{a}\mathbf{b}^\top + \mathbf{b}\mathbf{a}^\top) \quad (29)$$

$$\text{vec} \left(\frac{\partial^2 I_6}{\partial \mathbf{F}^2} \right) = (\mathbf{a}\mathbf{b}^\top + \mathbf{b}\mathbf{a}^\top) \otimes \mathbf{I}_{3 \times 3}. \quad (30)$$

The main challenge in an invariant-based eigenanalysis is usually locating a closed-form expression for the eigensystem of the invariant's Hessian, $\frac{\partial^2 I_6}{\partial \mathbf{F}^2}$. In this case, the Hessian has a regular, sparse structure, so the eigensystem is relatively straightforward:

$$\mathbf{Q}_0 = \begin{bmatrix} (\mathbf{a} + \mathbf{b})^\top \\ 0 & 0 \\ 0 & 0 \end{bmatrix} \quad \mathbf{Q}_1 = \begin{bmatrix} 0 & 0 \\ (\mathbf{a} + \mathbf{b})^\top \\ 0 & 0 \end{bmatrix} \quad \mathbf{Q}_2 = \begin{bmatrix} 0 & 0 \\ 0 & 0 \\ (\mathbf{a} + \mathbf{b})^\top \end{bmatrix}$$

$$\mathbf{Q}_3 = \begin{bmatrix} (\mathbf{a} - \mathbf{b})^\top \\ 0 & 0 \\ 0 & 0 \end{bmatrix} \quad \mathbf{Q}_4 = \begin{bmatrix} 0 & 0 \\ (\mathbf{a} - \mathbf{b})^\top \\ 0 & 0 \end{bmatrix} \quad \mathbf{Q}_5 = \begin{bmatrix} 0 & 0 \\ 0 & 0 \\ (\mathbf{a} - \mathbf{b})^\top \end{bmatrix}$$

$$\lambda_{0,1,2} = \mathbf{a}^\top \mathbf{b} + 1 \quad \lambda_{3,4,5} = \mathbf{a}^\top \mathbf{b} - 1. \quad (31)$$

If \mathbf{a} and \mathbf{b} are normalized and $\mathbf{a} \neq \mathbf{b}$, the last three eigenvalues are *always negative*.

With an invariant's eigensystem in hand, constructing the eigensystem of an energy that uses it (e.g. Ψ_{shear}) is usually straightforward. The Hessian of the overall energy is a scaled and rank-one updated version of the invariant's Hessian,

$$\text{vec} \left(\frac{\partial^2 \Psi_{\text{shear}}}{\partial \mathbf{F}^2} \right) = 2I_6 \mathbf{H}_6 + 2\mathbf{g}_6 \mathbf{g}_6^\top, \quad (32)$$

where

$$\mathbf{g}_6 = \text{vec} \left(\frac{\partial I_6}{\partial \mathbf{F}} \right) \quad \mathbf{H}_6 = \text{vec} \left(\frac{\partial^2 I_6}{\partial \mathbf{F}^2} \right). \quad (33)$$

This construction has been simple in previous work [KDG19, SGK18] because an invariant's gradient and Hessian have always been mutually orthogonal, i.e. $\mathbf{H}_6 \mathbf{g}_6 = 0$. However, this assumption *no longer holds* for $I_6(\mathbf{a}, \mathbf{b})$, because \mathbf{a} and \mathbf{b} are arbitrary directions that can produce non-zero projections onto the span of \mathbf{H}_6 . Thus, a new analysis is needed.

4.3.2. The Eigensystem of Baraff-Witkin Shearing

We perform a detailed, generalized analysis of shearing energies in Appendix B, where we use the Bunch-Nielsen-Sorensen (BNS) formulas [BNS78] to obtain closed-form expressions for the eigensystem. The derivation is involved, and the final expressions unwieldy, but we will now show that they simplify considerably in the Baraff-Witkin case.

Baraff-Witkin shearing corresponds to the case of $\mathbf{a} = \mathbf{a}_u$ and $\mathbf{b} = \mathbf{a}_v$. In this case, the eigenvalues from Eqn. 50 simplify to:

$$\lambda_0 = I_2 + \sqrt{I_2^2 + 12 \cdot I_6^2} \quad \lambda_{1,2} = I_6 \quad (34)$$

$$\lambda_3 = I_2 - \sqrt{I_2^2 + 12 \cdot I_6^2} \quad \lambda_{4,5} = -I_6. \quad (35)$$

The eigenvectors from Eqn. 52 become:

$$\mathbf{Q}_0 = I_6 \frac{\partial^2 I_6}{\partial \mathbf{F}^2} : \frac{\partial I_6}{\partial \mathbf{F}} + \lambda_0 \frac{\partial I_6}{\partial \mathbf{F}} \quad (36)$$

$$\mathbf{Q}_{1,2} = \begin{cases} \text{subspace of } \begin{bmatrix} 1 & 1 \\ 0 & 0 \\ 0 & 0 \end{bmatrix} \begin{bmatrix} 0 & 0 \\ 1 & 1 \\ 0 & 0 \end{bmatrix} \begin{bmatrix} 0 & 0 \\ 0 & 0 \\ 1 & 1 \end{bmatrix} \\ \text{orthogonal to } \mathbf{Q}_0 \end{cases} \quad (37)$$

$$\mathbf{Q}_3 = I_6 \frac{\partial^2 I_6}{\partial \mathbf{F}^2} : \frac{\partial I_6}{\partial \mathbf{f}} + \lambda_3 \frac{\partial I_6}{\partial \mathbf{f}} \quad (38)$$

$$\mathbf{Q}_{4,5} = \begin{cases} \text{subspace of } \begin{bmatrix} 1 & -1 \\ 0 & 0 \\ 0 & 0 \end{bmatrix} \begin{bmatrix} 0 & 0 \\ 1 & -1 \\ 0 & 0 \end{bmatrix} \begin{bmatrix} 0 & 0 \\ 0 & 0 \\ 1 & -1 \end{bmatrix} \\ \text{orthogonal to } \mathbf{Q}_3 \end{cases} \quad (39)$$

The shearing Hessian *always* has a rank-three negative-definite subspace. Two eigenvalues are persistently negative: $\lambda_{4,5} = -I_6$. The third negative eigenvalue, $\lambda_3 = I_2 - \sqrt{I_2^2 + 12 \cdot I_6^2}$, comes closest to positive when $12 \cdot I_6^2 = 0$, but only yields $\lambda_3 = I_2 - \sqrt{I_2^2} = 0$. The subspace is still semi-negative-definite, so the Baraff-Witkin shearing energy is *always indefinite*.

4.3.3. Semi-Positive-Definite Projection

We could compute the semi-positive-definite projection by explicitly constructing the positive eigenpairs and then summing their outer products, but this would involve robustly orthogonalizing the positive-definite subspace against \mathbf{Q}_0 .

Instead, we can avoid orthogonalization entirely. The positive-definite subspace from \mathbf{H}_6 is trivial to construct, $\mathbf{T} = \mathbf{1}_{2 \times 2} \otimes \mathbf{I}_{3 \times 3}$, where $\mathbf{1}_{2 \times 2}$ is a matrix of ones. Using this, we instead zero out the existing component in the $\text{vec}(\mathbf{Q}_0) = \mathbf{q}_0$ direction, and then add it back, scaled by λ_0 . More explicitly:

$$\mathbf{T} = \begin{bmatrix} 1 & \text{sign}(I_6) \\ \text{sign}(I_6) & 1 \end{bmatrix} \otimes \mathbf{I}_{3 \times 3} \quad (40)$$

$$\mathbf{H}_{\text{shear}}^+ = \|I_6\| \left(\mathbf{T} - \frac{1}{\|\mathbf{T}\mathbf{q}_0\|_2^2} \mathbf{T}\mathbf{q}_0\mathbf{q}_0^\top \mathbf{T}^\top \right) + \lambda_0 \mathbf{q}_0 \mathbf{q}_0^\top. \quad (41)$$

The $\text{sign}(I_6)$ and $\|I_6\|$ terms are included to handle the cases where $I_6 < 0$. The final semi-positive-definite version of the Baraff-Witkin shearing Hessian is then $\mathbf{H}_{\text{shear}}^+$. A complete C++ implementation is given in Appendix A.

5. Discussion and Experiments

The persistent indefiniteness of Ψ_{shear} is slightly surprising. The overall system is usually semi-positive definite; enough so that the original paper [BW98] did not even mention the possibility of indefiniteness. The negative eigenvalues are all $-I_6$, so it is possible that cloth-like stiffnesses prevent this term from becoming too large. It is also possible that the positive stretching eigenvalues, combined with the regularizing effects of the mass-inertia terms, tend to cancel this negative-definiteness.

We have verified the equivalence of our FEM formulation to the original formulation both numerically and qualitatively. First,



Figure 2: **Left:** Stretch test using original Baraff-Witkin force formulation [BW98]. **Center:** Stretch test, using our FEM formulation. The results are identical to the original. **Right:** Stretch test using ARAP instead of the original Baraff-Witkin stretching term. The results are qualitatively similar, but not identical. The lack of an explicit weft slightly suppresses horizontal wrinkling along the top and bottom.



Figure 3: **Left:** Same stretch test as Fig. 2, but without a shearing term. The wrinkles disappear entirely. **Center:** Our generalized Baraff-Witkin model from §5 with $\mathbf{b} = [1 \ 1]^\top$. **Right:** Our generalized Baraff-Witkin with $\mathbf{b} = [3 \ 1]^\top$. Altering \mathbf{b} significantly alters wrinkle formation. In all cases, $k = 100$ and the bending constant is $1e^{-4}$.

we confirmed that our forces and force gradients match the original forces up to working precision ($1e^{-8}$) for random values of \mathbf{F} . Then, we confirmed that simulations using both models produce the exact same results (Fig. 2, left and middle). All of our simulations are quasistatic; the shapes arise solely due to boundary conditions and material and gravity forces.

Given the similarity between Ψ_{stretch} and Ψ_{ARAP} , we also ran tests using Ψ_{ARAP} (Fig. 1 and Fig. 2, right). As expected, the results are qualitatively similar, but in Fig. 1, the ARAP version slightly suppresses higher-frequency wrinkles, and also favors a characteristic low-frequency wrinkle down the middle. In Fig. 2, the ARAP model is slightly more reluctant to wrinkle at the edges. In both cases, this makes ARAP appear more rubber-like. The same phenomenon appears when we perform a drape test (Fig. 4, left and middle). We speculate that these arise due to the absence of preferred warp and weft directions in the stretching energy.

With the equivalence established, we experimented with different variations on the original Baraff-Witkin energy. All of these experiments were run on a 40,000 vertex mesh with gravity set to $\mathbf{g} = [0 \ -9.8 \ 0]^\top$ and using the Discrete Shells bending energy [GHDS03]. The bending constant in Fig. 1 refers to the k_θ in $\Psi_\theta = k_\theta \frac{3l^2}{a} (\theta - \theta_0)^2$, where l , a , and θ_0 refer to the rest edge length, area, and bending angle. When the shearing term Ψ_{shear} is omitted from the simulation, wrinkling under extension disappears entirely (Fig. 3, left). The I_6 invariant clearly plays a critical role in the characteristic appearance of cloth.

We also experimented with relaxing the orthogonality conditions in the stretching and shearing energies, i.e. what happens when

$\mathbf{a} \neq \mathbf{a}_u$ and $\mathbf{b} \neq \mathbf{a}_v$? Non-orthogonal directions can be plugged directly into Ψ_{stretch} without any modification, but the shearing energy requires a more generalized form:

$$\Psi_{\text{general}} = a \left(I_6(\mathbf{a}, \mathbf{b}) - \mathbf{a}^\top \mathbf{b} \right)^2. \quad (42)$$

The original Ψ_{shear} tries to persistently restore the original angle between \mathbf{a}_u and \mathbf{a}_v , but since $\mathbf{a}_u^\top \mathbf{a}_v = 0$, it requires no explicit statement. For general \mathbf{a} and \mathbf{b} , the $\mathbf{a}^\top \mathbf{b}$ scalar must be introduced.

We set $\mathbf{a} = [1 \ 0]^\top$, but then set $\mathbf{b} = [1 \ 1]^\top$ and $\mathbf{b} = [3 \ 1]^\top$ in Fig. 3. In both cases, \mathbf{b} is normalized, and the wrinkles appear in progressively non-orthogonal directions, consistent with the weft direction specified by the new \mathbf{b} .

Higher-order versions of the Baraff-Witkin energies also suggest themselves. An StVK-like stretching term would be:

$$\Psi_{\text{stretch, StVK}} = a \left[\left(\sqrt{I_5(\mathbf{a}_u)} - b_u \right)^4 + \left(\sqrt{I_5(\mathbf{a}_v)} - b_v \right)^4 \right]. \quad (43)$$

However this energy is already mentioned and discarded in the original [BW98] paper (§4.2, first paragraph) as needlessly non-linear. An StVK-like shearing term also naturally suggests itself:

$$\Psi_{\text{shear, StVK}} = a \left(I_6(\mathbf{a}, \mathbf{b}) - \mathbf{a}^\top \mathbf{b} \right)^4. \quad (44)$$

Under stretching, this energy produces results that are qualitatively identical to the original shearing, but under draping, suppresses wrinkling altogether (Fig. 4, right).

Finally, we experimented with the effect of using our semi-



Figure 4: **Left:** Drape test using our FEM formulation of the Baraff-Witkin energy. **Middle:** Same test, using Ψ_{ARAP} in place of $\Psi_{stretch}$. The wrinkles near the edges are slightly suppressed, giving it a more rubbery appearance. **Right:** Same test, using $\Psi_{shear, SVK}$. The wrinkles are suppressed entirely. Here, $k = 30$, and the bending constant is $5e^{-7}$.

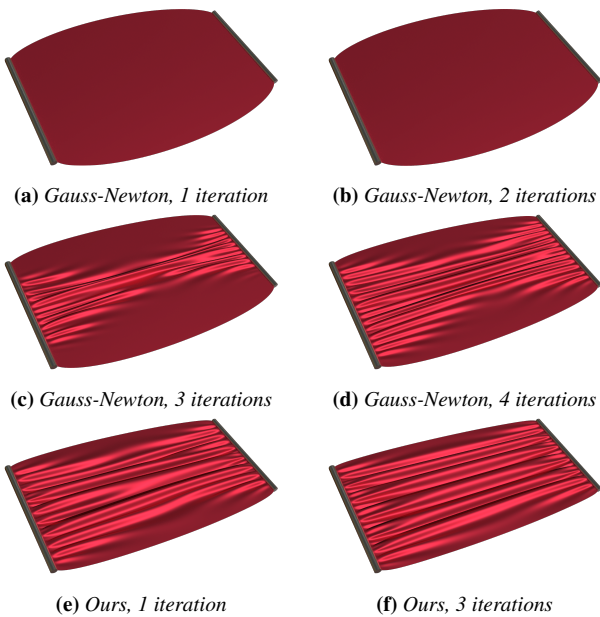


Figure 5: Stretch test, without gravity, with a Gauss-Newton approximation [CK02], has still not converged after 4 Newton iterations. Our approach is nearly converged after a single iteration.

positive-definiteness projection compared to the Gauss-Newton approach [CK02] of dropping all the \mathbf{H}_* terms. Fig. 5 shows the same scene as Figs. 2 and 3, but without gravity. A single Gauss-Newton iteration fails to capture any of the buckling features; they gradually appear after three Newton iterations. Using our approach, the features are nearly converged after a single iteration.

6. Conclusions and Future Work

We have presented an FEM formulation of Baraff-Witkin cloth using the I_5 and I_6 invariants. We have presented a novel analysis of I_6 , which is generally applicable, even outside of this context. Additionally, we have completely characterized the eigensystem of the model, including when the system becomes indefinite.

The effects of the positive-definiteness projection are worth further consideration. Indefiniteness indicates that multiple energetically enticing solutions are accessible from the current configuration, and the projection serves as a tie-breaker. What is the global effect of this tie-breaking? Does it sometimes bias the simulation towards energetically inferior states? Other strategies will almost certainly produce different results, particularly in the presence of collisions, and may be worth further investigation.

One future direction is to apply these results in a homogenization context [SNW20], as a granular mechanism now exists for encoding an arbitrary number of fiber-level directions. Finally, in light of the persistently indefinite shearing term, the question arises: does a qualitatively similar, more convex energy exist?

Acknowledgements

The author would like to thank Fernando de Goes and David Eberle for early discussions, as well as Julian Panetta for sharing the results of his membrane analysis.

Appendix A: C++ Code for Stretching and Shearing Hessians

This is a C++ implementation using Eigen [GJ*10] of the semi-definite projection from §4.2.2 for the stretch Hessian. Excluding spaces, comments, and typedefs, it is 19 lines of code.

```
typedef Eigen::Matrix<double, 2, 1> Vector2;
typedef Eigen::Matrix<double, 3, 1> Vector3;
typedef Eigen::Matrix<double, 3, 2> Matrix3x2;
typedef Eigen::Matrix<double, 6, 6> Matrix6x6;

void stretchHessian(const Matrix3x2 &F, Matrix6x6 &H) const
{
    H.setZero();
    const Vector2 u(1.0, 0.0);
    const Vector2 v(0.0, 1.0);
    const double I5u = (F * u).transpose() * (F * u);
    const double I5v = (F * v).transpose() * (F * v);
    const double invSqrtI5u = 1.0 / sqrt(I5u);
    const double invSqrtI5v = 1.0 / sqrt(I5v);

    // set the block diagonals, build the rank-three
    // subspace with all-(1 / invSqrtI5) eigenvalues
    H(0,0) = H(1,1) = H(2,2) = std::max((1.0 - invSqrtI5u), 0.0);
    H(3,3) = H(4,4) = H(5,5) = std::max((1.0 - invSqrtI5v), 0.0);

    // modify the upper block diagonal, bump the single
    // outer-product eigenvalue back to just 1, unless it
    // was clamped, then just set it directly to 1
```

```

const Vector3 fu = F.col(0).normalized();
const double uCoeff = (1.0 - invSqrtI5u >= 0.0) ? invSqrtI5u : 1.0;
H.block<3,3>(0,0) += uCoeff * (fu * fu.transpose());

// modify the lower block diagonal similarly
const Vector3 fv = F.col(1).normalized();
const double vCoeff = (1.0 - invSqrtI5v >= 0.0) ? invSqrtI5v : 1.0;
H.block<3,3>(3,3) += vCoeff * (fv * fv.transpose());

// the leading 2 is absorbed by the mu / 2 coefficient
H *= _mu;
}
    
```

This is a complete C++ implementation of the semi-positive-definite projection method from §4.3.3 for the Hessian of Ψ_{shear} . Excluding spaces and comments, it is 20 lines of code.

```

void shearHessian(const Matrix3x2 &F, Matrix6x6 &pPpF) const
{
    const Vector2 u(1.0, 0.0);
    const Vector2 v(0.0, 1.0);
    const double I6 = (F * u).transpose() * (F * v);
    const double signI6 = (I6 >= 0) ? 1.0 : -1.0;

    Matrix6x6 H = Matrix6x6::Zero();
    H(3,0) = H(4,1) = H(5,2) = H(0,3) = H(1,4) = H(2,5) = 1.0;

    const Vector6 g = flatten(F * (u * v.transpose() + v * u.transpose()));

    // get the novel eigenvalue
    const double I2 = F.squaredNorm();
    const double lambda0 = 0.5 * (I2 + sqrt(I2 * I2 + 12.0 * I6 * I6));

    // get the novel eigenvector
    // the H multiply is a column swap; could be optimized more
    const Vector6 q0 = (I6 * H * g + lambda0 * g).normalized();

    Matrix6x6 T = Matrix6x6::Identity();
    T = 0.5 * (T + signI6 * H);

    const Vector6 Tq = T * q0;
    const double normTq = Tq.squaredNorm();

    pPpF = fabs(I6) * (T - (Tq * Tq.transpose()) / normTq) +
        lambda0 * (q0 * q0.transpose());

    // half from mu and leading 2 on Hessian cancel
    pPpF *= _mu;
}
    
```

Finally, `flatten` implements `vec(·)` as follows:

```

Vector6 flatten(const Matrix3x2 &A) const
{
    Vector6 column;
    unsigned int index = 0;
    for (unsigned int j = 0; j < 2; j++)
        for (unsigned int i = 0; i < 3; i++, index++)
            column[index] = A(i, j);

    return column;
}
    
```

Appendix B: An Eigenanalysis of Generalized Shearing

In the following, we will perform a novel analysis of Ψ_{shear} for general \mathbf{a} and \mathbf{b} , and obtain some relatively unwieldy (but analytic) eigenvalues. The expressions become much simpler when we specialize to the Baraff-Witkin case in §4.3.2.

The Bunch-Nielsen-Sorensen (BNS) formulas [BNS78] can be used to quickly determine the eigendecomposition of a rank-one updated system, provided that the decomposition of the original system is already known. Similar to the related Sherman-Morrison-Woodbury formula [JP03], the approach is usually applied *numerically*, but the system we are examining is sufficiently small that we can apply the approach analytically.

From Eqn. 32, our original system is $I_6 \mathbf{H}_6$ (we drop the leading

2 for brevity), so its eigenvalues are a scaled version of Eqn. 31:

$$\lambda_{0,1,2} = I_6 (\mathbf{a}^T \mathbf{b} + 1) \quad \lambda_{3,4,5} = I_6 (\mathbf{a}^T \mathbf{b} - 1). \quad (45)$$

The next step in BNS is to project the normalized, rank-one update vector \mathbf{g}_6 into the eigenspace of the original system, i.e. \mathbf{Q} from $I_6 \mathbf{H}_6 = \mathbf{Q} \Lambda \mathbf{Q}^T$. We denote this projection as,

$$\mathbf{z} = \mathbf{Q}^T \frac{\mathbf{g}_6}{\|\mathbf{g}_6\|}, \quad (46)$$

where \mathbf{Q} in this case has the compact form (shown unnormalized):

$$\mathbf{Q} = \left[\begin{array}{c|c} \mathbf{a} + \mathbf{b} & \mathbf{a} - \mathbf{b} \end{array} \right] \otimes \mathbf{I}_{3 \times 3}. \quad (47)$$

Using this vector, we can now form the *secular equation* [Gol73]:

$$1 + \|\mathbf{g}_6\|^2 \sum_{i=0}^5 \left(\frac{z_i^2}{\lambda_i - \lambda} \right) = 0, \quad (48)$$

where z_i denotes the scalar entries of \mathbf{z} , and λ_i are the original eigenvalues of $I_6 \mathbf{H}_6$. For Eqn. 32, this becomes:

$$1 + \|\mathbf{g}_6\|^2 \left(\frac{z_0^2 + z_1^2 + z_2^2}{I_6 (\mathbf{a}^T \mathbf{b} - 1) - \lambda} + \frac{z_3^2 + z_4^2 + z_5^2}{I_6 (\mathbf{a}^T \mathbf{b} + 1) - \lambda} \right) = 0. \quad (49)$$

The λ roots correspond to the eigenvalues of the rank-one updated system we are interested in. The secular equation usually generates higher-order polynomials that must be solved numerically, but our original system only contained two unique eigenvalues, so Eqn. 49 is quadratic. Four of the six original eigenvalues remain exactly the same, and we only need to locate two new eigenvalues.

The roots of the quadratic can be solved for analytically to obtain the new eigenvalues:

$$\lambda_{0,3} = \alpha \pm \sqrt{\alpha^2 - 4I_6 [(\mathbf{a}^T \mathbf{b}^2 - 1)I_6 + \mathbf{a}^T \mathbf{b}I_2 - \beta]}. \quad (50)$$

where

$$\alpha = 2\mathbf{a}^T \mathbf{b}I_6 + I_2$$

$$\beta = \frac{\partial I_6}{\partial \mathbf{F}} \left[\begin{array}{c|c} \mathbf{a} + \mathbf{b} & \mathbf{a} - \mathbf{b} \end{array} \right] : \frac{\partial I_6}{\partial \mathbf{F}} \left[\begin{array}{c|c} \mathbf{a} + \mathbf{b} & \mathbf{b} - \mathbf{a} \end{array} \right]$$

We can alternatively state $\beta = (z_0^2 + z_1^2 + z_2^2) - (z_3^2 + z_4^2 + z_5^2)$, but the term remains unwieldy.

With the new eigenvalues in hand, the BNS formulas provide a simple means of computing the updated eigenvectors:

$$\mathbf{q}_{\text{new}} = \mathbf{Q} (\Lambda - \lambda_{\text{new}} \mathbf{I}_{6 \times 6})^{-1} \mathbf{Q}^T \mathbf{g}_6. \quad (51)$$

The structure of the eigenvalues in our problem allows the inverse to be pushed to an inner negation, reducing our case to the following eigenmatrices:

$$\mathbf{Q}_{0,3} = \frac{\partial^2 \Psi_{\text{sh}}}{\partial \mathbf{F}^2} : \frac{\partial I_6}{\partial \mathbf{F}} + \lambda_{0,3} \frac{\partial I_6}{\partial \mathbf{F}}. \quad (52)$$

The two new non-trivial eigenpairs for shearing are now fully specified by Eqns. 50 and 52. Each of these eigenpairs take the place of one eigenpair from the positive- and negative-definite subspaces for I_6 described in Eqn. 31.

The four remaining eigenvalues are unaltered from $I_6 \mathbf{H}_6$, and their eigenvectors now form two rank-two subspaces. The first spans the positive-definite subspace that is orthogonal to the new $(\lambda_0, \mathbf{Q}_0)$ eigenpair, and the second spans the negative-definite subspace orthogonal to $(\lambda_3, \mathbf{Q}_3)$. As in the stretching case, we see in §4.3.3 that explicit expressions for these subspaces are not needed to compute a semi-positive-definite projection. All of these expressions simplify when specialized to the Baraff-Witkin (§4.3.2).

References

- [BFA02] BRIDSON R., FEDKIW R., ANDERSON J.: Robust treatment of collisions, contact and friction for cloth animation. In *Proceedings of SIGGRAPH* (2002), pp. 594–603. 2
- [BML*14] BOUAZIZ S., MARTIN S., LIU T., KAVAN L., PAULY M.: Projective dynamics: fusing constraint projections for fast simulation. *ACM Trans. Graph.* 33, 4 (2014). 2
- [BM0*14] BENDER J., MÜLLER M., OTADUY M. A., TESCHNER M., MACKLIN M.: A survey on position-based simulation methods in computer graphics. *Comput. Graph. Forum* 33, 6 (Sept. 2014), 228–251. 2
- [BNS78] BUNCH J. R., NIELSEN C. P., SORENSEN D. C.: Rank-one modification of the symmetric eigenproblem. *Numerische Mathematik* 31, 1 (1978), 31–48. 1, 5, 8
- [BPD05] BLEMKER S. S., PINSKY P. M., DELP S. L.: A 3d model of muscle reveals the causes of nonuniform strains in the biceps brachii. *Journal of biomechanics* 38, 4 (2005), 657–665. 1, 3
- [BW98] BARAFF D., WITKIN A.: Large steps in cloth simulation. In *Proceedings of SIGGRAPH* (1998), p. 43–54. 1, 2, 5, 6
- [BW08] BONET J., WOOD R. D.: *Nonlinear continuum mechanics for finite element analysis*. Cambridge university press, 2008. 1, 2
- [CDH01] CRISCIONE J. C., DOUGLAS A. S., HUNTER W. C.: Physically based strain invariant set for materials exhibiting transversely isotropic behavior. *Journal of the Mechanics and Physics of Solids* 49, 4 (2001), 871–897. 1
- [CK02] CHOI K.-J., KO H.-S.: Stable but responsive cloth. In *Proceedings of SIGGRAPH* (2002), p. 604–611. 1, 2, 4, 7
- [CPSS10] CHAO I., PINKALL U., SANAN P., SCHRÖDER P.: A simple geometric model for elastic deformations. *ACM Trans. Graph.* 29, 4 (2010), 1–6. 3
- [CRF15] CHAGNON G., REBOUAH M., FAVIER D.: Hyperelastic energy densities for soft biological tissues: a review. *Journal of Elasticity* 120, 2 (2015), 129–160. 3
- [CSvRV18] CHEN H.-Y., SASTRY A., VAN REES W. M., VOUGA E.: Physical simulation of environmentally induced thin shell deformation. *ACM Trans. Graph.* 37, 4 (July 2018). 2
- [CTT17] CLYDE D., TERAN J., TAMSTORF R.: Modeling and data-driven parameter estimation for woven fabrics. In *Proceedings of the ACM SIGGRAPH/Eurographics Symposium on Computer Animation* (2017). 2
- [Ebe18] EBERLE D.: Better collisions and faster cloth for pixar’s coco. In *ACM SIGGRAPH Talks* (2018). 1
- [EKS03] ETZMUSS O., KECKEISEN M., STRASSER W.: A fast finite element solution for cloth modelling. In *Proceedings of Pacific Graphics* (2003), IEEE, pp. 244–251. 2
- [GHDS03] GRINSPUN E., HIRANI A. N., DESBRUN M., SCHRÖDER P.: Discrete shells. In *Proceedings of the ACM SIGGRAPH/Eurographics Symposium on Computer Animation* (2003), p. 62–67. 6
- [GJ*10] GUENNEBAUD G., JACOB B., ET AL.: Eigen v3. <http://eigen.tuxfamily.org>, 2010. 7
- [Gol73] GOLUB G. H.: Some modified matrix eigenvalue problems. *Siam Review* 15, 2 (1973), 318–334. 8
- [GVL13] GOLUB G. H., VAN LOAN C. F.: *Matrix computations*. The Johns Hopkins University Press (2013). 3
- [JP03] JAMES D. L., PAI D. K.: Multiresolution green’s function methods for interactive simulation of large-scale elastostatic objects. *ACM Trans. Graph.* 22, 1 (Jan. 2003), 47–82. 8
- [KDG19] KIM T., DE GOES F., IBEN H.: Anisotropic elasticity for inversion-safety and element rehabilitation. *ACM Trans. Graph.* 38, 4 (July 2019). 1, 2, 3, 4, 5
- [LB15] LI Y., BARBIĆ J.: Stable anisotropic materials. *IEEE Trans. on Vis. and Comp. Graph.* 21, 10 (2015), 1129–1137. 2
- [LZX*08] LIU L., ZHANG L., XU Y., GOTSMAN C., GORTLER S. J.: A local/global approach to mesh parameterization. In *Proceedings of the Symposium on Geometry Processing* (2008), p. 1495–1504. 3
- [MBT*12] MIGUEL E., BRADLEY D., THOMASZEWSKI B., BICKEL B., MATUSIK W., OTADUY M. A., MARSCHNER S.: Data-driven estimation of cloth simulation models. *Computer Graphics Forum* 31, 2pt2 (2012), 519–528. 2
- [MFG09] MATHIS, FISHBOY82, GREGORIUS D.: Baraff/witkin’s integration matrix not positive: what to do?, 2009. URL: <https://pybullet.org/Bullet/phpBB3/viewtopic.php?t=4350>. 1, 2
- [MHR07] MÜLLER M., HEIDELBERGER B., HENNIX M., RATCLIFF J.: Position based dynamics. *Journal of Visual Communication and Image Representation* 18, 2 (2007), 109–118. 1, 2
- [MMO16] MIGUEL E., MIRAUT D., OTADUY M. A.: Modeling and estimation of energy-based hyperelastic objects. In *Proceedings of Eurographics* (2016), p. 385–396. 2
- [NOB16] NARAIN R., OVERBY M., BROWN G. E.: ADMM \supseteq Projective Dynamics: Fast Simulation of General Constitutive Models. In *Proceedings of the ACM SIGGRAPH/Eurographics Symposium on Computer Animation* (2016). 2
- [Pan20] PANETTA J.: Analytic eigensystems for isotropic membrane energies, 2020. [arXiv:2008.10698](https://arxiv.org/abs/2008.10698). 4
- [Pro95] PROVOT X.: Deformation constraints in a mass-spring model to describe rigid cloth behaviour. In *Graphics interface* (1995). 2
- [SA07] SORKINE O., ALEXA M.: As-rigid-as-possible surface modeling. In *Proceedings of the Eurographics Symposium on Geometry Processing* (2007), p. 109–116. 1
- [SGK18] SMITH B., GOES F. D., KIM T.: Stable neo-hookean flesh simulation. *ACM Trans. Graph.* 37, 2 (Mar. 2018). 1, 5
- [SGK19] SMITH B., GOES F. D., KIM T.: Analytic eigensystems for isotropic deformation energies. *ACM Trans. Graph.* 38, 1 (Feb. 2019). 3
- [SNW20] SPERL G., NARAIN R., WOJTAN C.: Homogenized yarn-level cloth. *ACM Trans. Graph.* (2020). 7
- [TJM15] TAMSTORF R., JONES T., MCCORMICK S. F.: Smoothed aggregation multigrid for cloth simulation. *ACM Trans. Graph.* 34, 6 (Oct. 2015). 1
- [TPS09] THOMASZEWSKI B., PABST S., STRASSER W.: Continuum-based strain limiting. *Computer Graphics Forum* 28, 2 (2009), 569–576. 2
- [TSIF05] TERAN J., SIFAKIS E., IRVING G., FEDKIW R.: Robust quasi-static finite elements and flesh simulation. In *Proceedings of the ACM SIGGRAPH/Eurographics Symposium on Computer Animation* (2005), pp. 181–190. 2
- [VMTF09] VOLINO P., MAGNENAT-THALMANN N., FAURE F.: A simple approach to nonlinear tensile stiffness for accurate cloth simulation. *ACM Trans. Graph.* 28, 4 (Sept. 2009). 2
- [VT00] VOLINO P., THALMANN N. M.: Implementing fast cloth simulation with collision response. In *Proceedings Computer Graphics International* (2000), IEEE, pp. 257–266. 2
- [WOR11] WANG H., O’BRIEN F., RAMAMOORTHY R.: Data-driven elastic models for cloth: Modeling and measurement. *ACM Trans. Graph.* 30, 4 (July 2011), 71:1–11. 2